

PARAMETERIZATION OF INCOMING LONGWAVE RADIATION IN HIGH-MOUNTAIN ENVIRONMENTS

Matthias Gabathuler
Atmospheric Science
Swiss Federal Institute of Technology
ETH Hönggerberg
8093 Zürich
Switzerland

Christoph A. Marty
Physical Meteorological Observatory Davos
World Radiation Center
Dorfstrasse 33
7260 Davos
Switzerland

Kurt W. Hanselmann
University of Zürich
Institute of Plant Biology
Department of Microbiology
Zollikerstrasse 107
8008 Zürich
Switzerland

Abstract: Some ecological applications and energy budget calculations of the earth's surface require accurate estimates of incoming longwave radiation. As cloud cover observations are not conducted frequently in high-mountain environments, a new model for the parameterization of daily mean incoming longwave radiation is proposed based on global radiation instead of cloud cover. Besides global radiation, the new model requires data for air temperature, relative humidity, and an estimate of daily mean cloudless global radiation. The model was calibrated with data from high-mountain and lowland stations and the results are compared with existing models. The new model yielded consistent results under all cloud-cover conditions, for different sites, and for all seasons. For the conditions tested, the absolute mean bias error was generally less than 10 Wm^{-2} and the root mean square error was always between 11 Wm^{-2} and 16 Wm^{-2} . Of the other models tested, some did not perform well under cloudless conditions and others yielded large errors under overcast conditions or were not applicable to high mountain sites. The new model is a viable alternative to the existing longwave parameterization models, especially for high-mountain environments, and it can be applied without the resource-consuming observation of cloud cover. [Key words: longwave radiation, global radiation, cloud cover, high mountains, model.]

INTRODUCTION

The longwave components of the radiation budget are important elements for many geophysical and ecological applications. These include energy-budget calcu-

lations of lakes (Livingstone and Imboden, 1989), snowmelt models (Olyphant, 1986), glacier mass budgets (Greuell et al., 1997), build-up of radiation fog, and many more. The quantification of longwave radiation is necessary to correctly estimate the radiative heat losses of the systems mentioned above. Unlike global radiation, incoming longwave radiation, also known as atmospheric radiation, is not measured frequently at standard weather stations. The reason for this is that reasonably accurate global radiation measurements can be obtained with a low budget, whereas accurate longwave radiation measurements are still difficult to obtain. Therefore, longwave radiation data often have to be estimated based on empirical models. Another possibility would be to calculate incoming longwave radiation with fundamental physical models. These models attempt to describe the real emission and absorption processes that take place in the troposphere. Such models give excellent estimates of sky radiation, but require vertical profile data of temperature and humidity, both of which are generally not available, making these models useless for many applications. Empirical models are used more frequently, even though they are less precise than the fundamental models. The reason for this is that they can estimate incoming longwave radiation based on easier-to-measure surface meteorological measurements (Swinbank, 1963; Idso and Jackson, 1969; Brutsaert, 1975; Berdahl and Martin, 1984; Ineichen et al., 1984; Aubinet, 1994; Konzelmann et al., 1994).

A number of studies attempting to model atmospheric longwave radiation have focused on cloudless conditions. Cloudless days are the exception rather than the rule, however, in most climatic zones, which limits the applicability of many cloudless models. Most radiation models that include cloud cover were developed for lowland environments and are of limited use in high-mountain environments (e.g., Barry, 1992). Furthermore, existing radiation models strongly depend on cloud cover, a parameter whose measurement can hardly be achieved objectively and, in particular, cannot be measured by an automatic weather station. Consequently, an approach independent of cloud cover determinations was needed for high-mountain locations.

Since global radiation data are usually more reliable and easier to obtain than cloud cover, global radiation should be a viable substitute for cloud cover, if the parameterization of longwave radiation is adapted. Only a few researchers have tried to develop longwave radiation models that include global radiation instead of cloud cover data (Ineichen et al., 1984; Aubinet, 1994). Since the models of these authors were developed with data from lowland stations, their applicability to high-mountain environments is problematic.

None of the previously described models were tested rigorously for different cloud conditions, climatic zones, altitudes, or seasons. The results of this study will illustrate how some existing models produce weak results under certain specific conditions and how a newly designed model of incoming longwave radiation can overcome these shortcomings. Here we illustrate that the new method accurately describes incoming longwave radiation in high-mountain environments as well as in lowland environments, for all cloud conditions and seasons. The model is based on screen-level measurements of air temperature, humidity, and global radiation.

DATA AND MODEL DEVELOPMENT

Available Data Sets

Radiation budget measurements are conducted at several stations in the Swiss Alps within the Alpine Surface Radiation Budget (ASRB) project (Philipona et al., 1996; Marty, 2000). Incoming and outgoing global and longwave radiation are measured by the PMOD/WRC (Physical Meteorological Observatory Davos/World Radiation Center) and stored in two-minute intervals. The stations chosen for the development of the new model were Weissfluhjoch ($46^{\circ}50'04''$ N, $9^{\circ}48'27''$ E, 2693 m a.s.l.) and the Research Field of the Swiss Federal Institute for Snow and Avalanche Research (SLF) ($46^{\circ}49'49''$ N, $9^{\circ}48'38''$ E, 2544 m a.s.l.) in eastern Switzerland and Payerne ($46^{\circ}48'49''$ N, $6^{\circ}56'33''$ E, 490 m a.s.l.), a lowland station in western Switzerland. The lowland station was included to improve the model's suitability for lower altitudes as well.

Hereinafter, the data from these three stations will be referred to as "PMOD/WRC data set." PMOD/WRC data from Jungfraujoch ($46^{\circ}32'56''$ N, $7^{\circ}59'10''$ E, 3580 m a.s.l.) were used to verify the model. The standard ASRB instrumentation, mounted on an aluminum arm fixed on a mast about 5 m above ground, includes an Eppley PIR pyrgeometer for incoming longwave radiation and a Kipp & Zonen CM21 pyranometer for global radiation measurements. Both instruments are especially shielded and ventilated to guarantee reliable data even under harsh alpine conditions. Additionally, air temperature and humidity were measured at those sites with a THYGAN (Meteolabor, Switzerland). The THYGAN measures the air temperature and dew point temperature 10 times within 40 seconds, every 10 minutes. The instrument delivers the average values together with their standard deviations, allowing the quality of the data to be checked. Cloud cover was observed at the Weissfluhjoch, Payerne, and Jungfraujoch stations three times a day by the Swiss Meteorological Institute. These observations allowed for comparisons with longwave models including cloud coverage. Because of its proximity to the Weissfluhjoch, the cloud cover of the SLF Research Field was assumed to be equal to that of Weissfluhjoch, the distance between the two stations being less than one kilometer. The development and testing of the model was performed with conventionally calculated daily mean data of 1997. Because of the reliability of the instruments, none of the PMOD/WRC data had to be corrected in any way, except for excluding days when data losses had occurred.

Meteorological measurements including longwave radiation were also conducted at the Jöri Lakes ($46^{\circ}46'39''$ N, $9^{\circ}58'43''$ E, 2520 m) as part of the project MOLAR (Mountain Lake Research; Gabathuler, 1999). The Jöri site is located about 14 km southeast of the Weissfluhjoch site. Longwave radiation was measured with a pyrgeometer (Kipp & Zonen CG1), global radiation with a pyranometer (Kipp & Zonen CM6B), and temperature and relative humidity were measured 8 m above ground within the same multiplate shield, but the instruments were not artificially ventilated. The global radiation data were compared to data of a nearby station. When daily mean global radiation at the Jöri site was less than 70% of the radiation at the nearby station and snowfall was observed, then the data of that day were

erased, assuming a snow cover on the sensors. The data from the Jöri Lakes were used to verify the new model.

Model Development

The basic equation for most longwave radiation models is the Stefan-Boltzmann Law, which relates longwave radiation flux density (LW) to the absolute temperature (T) and the emissivity ϵ of the emitting object, such that

$$LW = \epsilon \sigma T^4 [Wm^{-2}], \quad (1)$$

where σ is the Stefan-Boltzmann constant ($5.67 \times 10^{-8} Wm^{-2}K^{-4}$). Application of this equation to the incoming longwave radiation at the earth's surface requires some modifications (Saunders and Bailey, 1997). The difficulties lie in the determination of the temperature T_a and the emissivity ϵ_a of the atmosphere. Most longwave radiation models (Swinbank, 1963; Idso and Jackson, 1969; Brutsaert, 1975; Konzelmann et al., 1994; and many others) relate effective emissivity of the atmosphere to air temperature, vapor pressure, and cloud cover.

The approach presented in this paper focuses less on the calculation of emissivity, but on the calculation of sky temperature. The sky temperature is assumed to be the equivalent radiative temperature at a sky emissivity ϵ_a of 1, which is equal to black-body emissivity. The idea behind this approach is that the difference between screen-level temperature and sky temperature is a function of the clearness index K_0 and the relative humidity RH.

The clearness index in this study is defined as

$$K_0 = \frac{H}{H_0}, \quad (2)$$

where H is the measured daily mean global radiation and H_0 is the theoretically possible daily mean cloudless global radiation on the same day. H_0 can be calculated using the formulas by Kondratyev (1973), which assume standard atmospheres with given turbidities for different months. Shading effects can be calculated by incorporating a digital elevation model. H_0 can also be approximated more empirically if a year's data set of global radiation for the site in question is available (see below). It is important not to ignore the shading effects of the skyline when calculating the daily mean cloudless radiation. Ignoring shading decreases the clearness index systematically, indicating cloud cover when there is none.

The empirical approximation of cloudless radiation with a year's data set of measured global radiation is based on values of days with little or no cloud cover. A five-day maximum of the measured global radiation is calculated for each day of the year. For every day where this calculated maximum global radiation is less than on the day before, the average between the last higher and the next higher values is considered to be the maximum. This approach is taken from 21 December to 21 June forward and backward in time. After these calculations, one should receive a data set of rising global radiation from 21 December to 21 June and of decreasing global radiation from 21 June to 21 December. To smooth the values, a 15-day mean value is calculated for each day. The resulting values are considered to be the

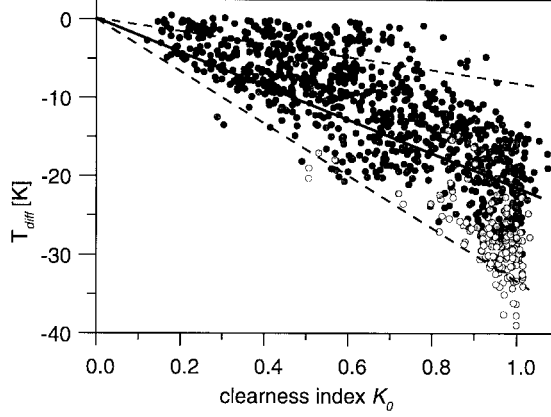


Fig. 1. The difference T_{diff} between air temperature and emission temperature of the sky as a function of the clearness index K_0 . The points are shaded according to the relative humidity, with empty and full circles representing relative humidity of less than 30% and more than 90%, respectively. Intermediate relative humidity values (between 30% and 90%) are differently shaded in 20% steps. The upper and lower dashed lines represent the linear regression of the dates, with more than 90% and less than 30% relative humidity, respectively. The solid line depicts the linear regression ($r^2 = 0.58$, $p < 0.05$) of the complete data set through the origin of the coordinate system ($T_{diff} = 0$ K for a clearness index of 0).

cloudless radiation for each day. The authors are aware that this approach is extremely empirical, but based on the following model calculations these data seem to be sufficiently accurate.

In a first step, the sky temperature was calculated from the actually measured incoming longwave radiation LW_{meas} , according to the Stefan-Boltzmann Law (Equation 1), assuming a sky emissivity ϵ_a of 1. Subsequently, the temperature difference T_{diff} between the recorded air temperature T_a and the sky temperature were calculated

$$T_{diff} = \sqrt[4]{\frac{LW_{meas}}{5.67 \times 10^{-8}}} - T_a. \quad (3)$$

The temperature difference between screen level and sky was plotted against the clearness index, with all the points being shaded according to the relative humidity (Fig. 1). The plot shows that at low relative humidity the clearness index tends to be high and the temperature difference large. The opposite can be said for days with high relative humidity. For a correlation between temperature difference and clearness index, a nonlinear approach would seem to be appropriate. However, as stated earlier, the difference between screen and sky temperature is not expected to be solely dependent on the clearness index, but also on humidity. Consequently, days with similar relative humidity were grouped and correlated independently. All humidity groups cluster around lines with a gradient dependent on the humidity. If, in a second step, a correction for relative humidity is made, it seems appropriate that a linear regression between clearness index and temperature difference over

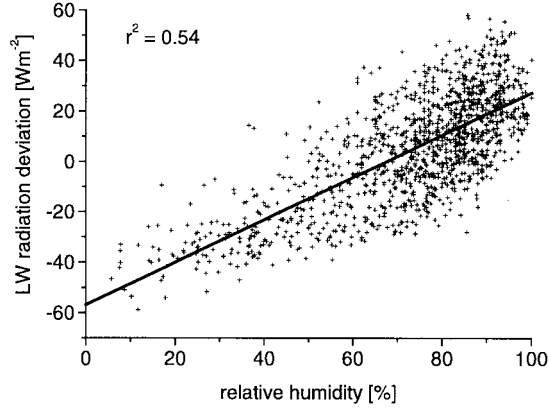


Fig. 2. Scatter plot between relative humidity and the difference between measured and parameterized incoming longwave radiation. The parameterization of incoming longwave radiation (Equation 4) does not include the correction factor for humidity. The line represents the linear regression of the data ($r^2 = 0.54$, $p < 0.05$). The slope and the intercept of the regression were used to correct the longwave parameterization for relative humidity.

the entire data set serves as a good basis for the model. The linear regression yielding a minimum standard deviation is the one with a sky temperature 21 K below surface temperature for cloudless conditions (clearness index of 1). This linear regression yields a correlation of $r^2 = 0.58$ for the complete data set, using 1071 measurements.

Based on this linear regression of the data set from the three stations (Fig. 1) one can approximate LW_{calc} as:

$$LW_{calc} = \sigma(-21 K_0 + T_a)^4 \quad (4)$$

The essential contribution of this equation is that the temperature difference T_{diff} for cloudless conditions ($K_0 = 1$) is expected to be -21 K. However, at low humidity, it can be as much as -41 K, as shown in Figure 1. For this reason, Equation (4) was optimized by adding a correction factor including relative humidity. Relative humidity was chosen because it leads to a much better linear regression when correlated with the difference between LW_{calc} (Equation 4) and LW_{meas} , as opposed to water vapor pressure. The correction factor was found through a linear regression between relative humidity and the deviation of the calculated longwave radiation (based on Equation 4) from the measured one (Fig. 2).

The final model for the calculation of incoming longwave radiation can therefore be presented as

$$LW_{calc} = (-21 K_0 + T_a)^4 \sigma + 0.84 RH - 57, \quad (5)$$

where RH is the relative humidity expressed as a percentage. Equation (5) can be algebraically transformed to fit the basic Equation (1):

Table 1. Longwave Radiation Models According to Several Authors Including the Model Introduced in This Study

Author	Equation ^a	Model
This study	$LW_{calc} = \left[\left(\frac{0.84(RH - 68)}{\sigma T_a^4} + \left(\frac{-21K_0}{T_a} + 1 \right)^4 \right) \right] \sigma T_a^4$	1
Konzelmann et al. (1994)	$LW_{calc} = \left[\left(0.23 + 0.483 \left(\frac{e_a}{T_a} \right)^{\frac{1}{8}} \right) (1 - n^3) + 0.963 n^3 \right] \sigma T_a^4$	2
Idso and Jackson (1969)	$LW_{calc} = (1 + 0.22n^2) \left(1 - 0.261 \exp^{-7.77 \times 10^{-4}(T_a - 273.15)} \right) \sigma T_a^4$	3
Brutsaert (1975)	$LW_{calc} = (1 + 0.22n^2) 0.642 \left(\frac{e_a}{T_a} \right)^{\frac{1}{7}} \sigma T_a^4$	4

^aAbbreviations: e_a = vapor pressure; T_a = air temperature; n = cloud cover; K_0 = clearness index; rh = relative humidity; σ = Stefan-Boltzmann constant.

$$LW_{calc} = \left(\frac{0.84(RH - 68)}{\sigma T_a^4} + \left(\frac{-21K_0}{T_a} + 1 \right)^4 \right) \sigma T_a^4, \quad (6)$$

with the expression in brackets being the atmospheric emissivity ϵ_a . On certain occasions, the calculated sky emissivity can be larger than 1. Measured emissivity was above unity on only three of the 1071 days, when low clouds prevailed above the measuring sites and owing to the fact that the atmosphere is not a black body. Therefore, because effective emissivity cannot be above 1, the sky emissivity was set to 1, when it was calculated to be above 1. This further improves the model.

RESULTS

Other Longwave Radiation Models

Three existing models were tested with the available data set of the PMOD/WRC (Table 1) and the results compared to the new model. The Idso and Jackson model (1969) is based on cloud cover (n) and air temperature (T_a) alone, while the other two (Brutsaert, 1975, Konzmann et al., 1994) also incorporate vapor pressure (e_a). The Idso-Jackson model was chosen to assess the performance of a model that does not include any humidity data. The Brutsaert approach is widely used for the parameterization of incoming longwave radiation in lake energy budget calcula-

Table 2. Comparative Statistics for the Complete Data Set and for the Data Sets of each PMOD/WRC-Station

Model	MBE				RMSE				r^2
	All ^a	SRF ^b	WFJ ^c	PAY ^d	All ^a	SRF ^b	WFJ ^c	PAY ^d	All ^a
1	-0.35	-0.71	4.29	-4.59	14.71	14.82	14.22	13.70	0.904
2	6.83	7.55	10.45	2.51	14.93	15.48	16.03	11.83	0.887
3	-0.15	4.69	8.06	-13.13	21.60	21.36	22.83	12.82	0.621
4	-11.19	-15.90	-13.57	-3.90	20.84	20.10	20.00	20.50	0.857

^aIndices for the complete PMOD/WRC data set ($n = 1071$).

^bIndices for the SLF Research Field data.

^cIndices for the Weissfluhjoch data.

^dIndices for the Payerne data.

tions (Marti and Imboden, 1986; Livingstone and Imboden, 1989; Liston and Hall, 1995). To assess the performance of an up-to-date model, the Konzelmann parameterization was included. The models of Idso and Jackson (1969) and Brutsaert (1975) were both developed for cloudless conditions. To make them suitable for cloudy skies, their equations were supplemented with a cloud correction factor (Bolz, 1949):

$$LW_{calc} = LW_0 (1 + a n^2), \quad (7)$$

where LW_0 is the cloudless longwave radiation, n is the proportion of cloud cover ($0 < n < 1$), and the variable a is dependent on cloud type. Oke (1987) assigned 0.22 to the variable a for conditions without cirroform clouds, while Brutsaert (1982) chose 0.17. Because of the high frequency of stratoform and cumuloform clouds compared to cirroform clouds in the high mountains, a value of 0.22 was chosen.

Overall Performance of the New Model

The performance of all models was evaluated for the complete PMOD/WRC data set and for the three measurement sites Weissfluhjoch, SLF Research Field, and Payerne individually. The calculations for each site yielded basic information on the suitability of the models for different climatic environments. The mean bias error (MBE) and the root mean square error (RMSE) of the linear regression between measured and modeled values were calculated (Table 2). The MBE represents the systematic error of the calculations over an entire season. Together with the RMSE the expected daily accuracy of the model calculations can be determined. A parameterization is suitable if the MBE is close to 0 Wm^{-2} and the RMSE is as small as possible.

LW_{calc} calculated with the new method (model 1) reached an r^2 of 0.90 for the complete PMOD/WRC data set (Table 3). Judging from the r^2 value, the new model

Table 3. Correlation between the Measured and the Calculated Incoming Longwave Radiation of the Four Tested Models and the Three Measuring Sites

Model Nr.	r^2 all ^a	r^2 SRF ^b	r^2 WFJ ^c	r^2 PAY ^d
1	0.90	0.87	0.88	0.85
2	0.89	0.83	0.80	0.90
3	0.62	0.38	0.21	0.85
4	0.86	0.79	0.78	0.82

^aComplete PMOD/WRC data set.

^bData set of SLF Research Field (2544 m a.s.l.).

^cData set of Weissfluhjoch (2693 m a.s.l.).

^dData set of Payerne (490 m a.s.l.).

describes the data best. The MBE for model 1 is expected to be close to zero since the model is based on the data it was tested on. The RMSE of model 1 is lowest and r^2 is highest of all the models applied to the complete data set. Model 2 (Konzelmann et al., 1994) is also in good agreement, with low RMSEs. The aforementioned authors presented their formula for daily mean longwave radiation based on measurements in the Arctic. Although the MBE of model 3 (Idso and Jackson, 1969) is small, the large RMSE makes this model less suitable for high-mountain environments. The r^2 is lowest for model 3, which reflects its inability to correctly model longwave radiation under cold and dry conditions, situations that are frequent in high-mountain regions. Taking into consideration the fact that model 3 only uses inputs of cloud cover and air temperature data, the general results are reasonably good. Model 4 (Brutsaert, 1975) yields reasonable results for the Payerne data set, but it cannot be applied to high-mountain conditions. Modeled longwave radiation is generally too low for the Brutsaert equation (Fig. 3, model 4). The data of the low-land site of Payerne is best modeled with model 2, closely followed by the new model. Models 3 and 4 have either unfavorable MBE or RMSE. The incoming longwave radiation of the high-mountain stations are clearly best described with the new model, followed by model 2. Models 3 and 4 are less suitable for the high mountain data; they yield a particularly high RMSE.

Error Analysis

An error analysis was performed on the complete data set and all the four models discussed. All input variables to the models were individually subjected to random errors with a maximum of $\pm 10\%$ for global radiation, maximum radiation, and cloud cover; a maximum of $\pm 5\%$ for relative humidity; and $\pm 1^\circ \text{C}$ for air temperature. The results proved to be similar for all stations, but differed slightly among the models. Because the averages after applying the random errors were close to the original average of all values, the changes in MBE can be neglected. An error in the radiation data obviously only leads to an increase in RMSE for model 1. The

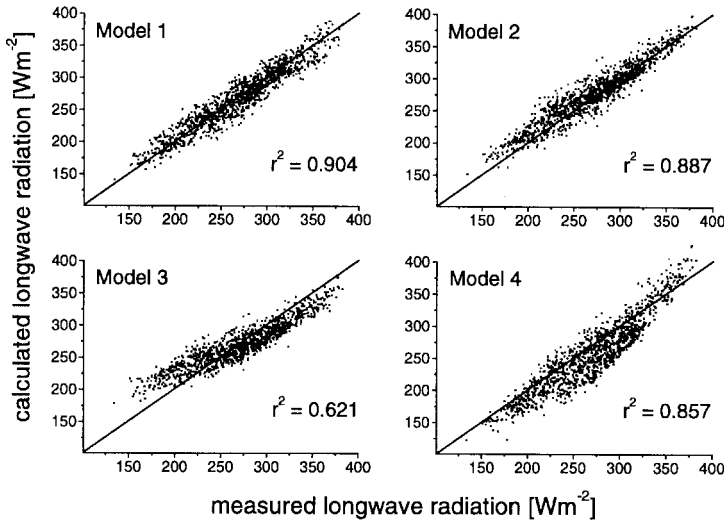


Fig. 3. Scatter plot between calculated and measured longwave radiation of the complete data set ($n = 1071$) in 1997 for all four models. The 1:1 line is displayed in all graphs. Model numbers correspond to the numbers in Table 1.

changes were moderate, with an average RMSE increase of 0.4 Wm^{-2} and 0.6 Wm^{-2} for global radiation and maximum radiation, respectively. The random errors applied to cloud cover yielded an increased RMSE of 1 Wm^{-2} for model 2 and only 0.3 Wm^{-2} for models 3 and 4. The effects of random errors in humidity and air temperature on the RMSE were very small for all models, with maximal changes of 0.2 Wm^{-2} .

It seems that all models are quite stable under the influence of random errors. Except for the reaction of model 2 to errors in cloud cover data, all RMSE changes were far below 1 Wm^{-2} .

Model Performance as a Function of Cloud Cover

The stability of each model was tested for different cloud cover percentages. The performance of the models was evaluated for calculated apparent sky emissivities ϵ_a (Table 4). A sky emissivity below 0.7 represents mostly clear skies (mean cloud cover of 20% for the PMOD/WRC data set), between 0.7 and 0.8 partly cloudy skies (mean cloud cover of 50% for the PMOD/WRC data set), and above 0.95 completely overcast skies.

The new model yields acceptable results for all cloud conditions with absolute MBE always below 10 Wm^{-2} and RMSE between 11 Wm^{-2} and 14 Wm^{-2} . The other models yield variable results for the three different cloud conditions tested. MBE is large for model 2 under cloudless conditions, while it parameterizes incoming longwave radiation with an absolute MBE of below 10 Wm^{-2} and an RMSE of less than 8 Wm^{-2} for overcast conditions. RMSE is even smaller under overcast condi-

Table 4. Comparative Statistics of the PMOD/WRC Data Set in Relation to Cloudiness (Emissivity ϵ_a)^a for All Four Models

Model	$\epsilon_a < 0.7$ ($n = 197$)		$0.7 < \epsilon_a < 0.8$ ($n = 238$)		$\epsilon_a > 0.95$ ($n = 150$)	
	MBE	RMSE	MBE	RMSE	MBE	RMSE
1	7.9	11.3	4.2	13.5	-8.7	13.7
2	21.4	10.6	12.0	13.7	-6.1	7.2
3	33.1	9.9	8.6	12.4	-23.9	5.2
4	-1.5	14.3	-3.6	15.7	-36.5	13.4

^aCalculated emissivity based on the measurements of longwave radiation and air temperature.

tions for model 3, but the corresponding MBE is far from 0 Wm^{-2} . The same is true for cloudless conditions. Model 3 only yields reasonable results for partly cloudy conditions. Model 4 yields good results under cloudless and partly cloudy skies. Brutsaert (1975) developed model 4 using only cloudless data. In fact, for days with a sky emissivity of less than 0.7, model 4 yields the smallest absolute MBE (Table 4), but since cloudless days are rare in most climatic zones, the equation's applicability is limited. For overcast conditions, absolute MBE is very large in model 4.

It seems that either the cloud cover correction factor (Equation (7)) proposed by Bolz (1949) or the corresponding cloud type indices as proposed by Oke (1987), which were applied to models 3 and 4, are unsuitable under the conditions of the PMOD/WRC data set. Analysis of the dependence between cloud cover and calculated incoming longwave radiation according to model 4 showed that the variable a in Equation (7) seems to be dependent on altitude. The Payerne data set would be best modeled with $a = 0.28$, the Weissfluhjoch and SLF Research Field data with $a = 0.37$, and the Jungfrauoch data with $a = 0.49$. These values are much higher than the values proposed by Oke (1987) and by Brutsaert (1982). The cloud correction factor of model 3 should be linear rather than quadratic in order to improve the model, as analyses have shown. Data from other altitudes or climatic zones should be employed to better define the value of the variable a .

Applying the Models to Independent Data Sets

In this section the performance of the four models (Table 1) applied to two independent data sets is described. One set of data was recorded at the shore of a mountain lake (Jöri Lakes, 2520 m a.s.l.), in the period between July 1996 and September 1999. The Jöri Lakes are 14 km from the Weissfluhjoch station and the SLF Research Field site. The cloud cover at the Jöri Lakes was assumed to correspond to those observed at the Weissfluhjoch site. The Jöri data set was collected during the years 1996 through 1998. Days on which the unventilated and unheated radiation sensors might have been covered with snow were not included, leaving a total of 753 data points for model verification. The other data set was recorded as part of the

Table 5. Comparative Statistics of the Data from the Independent Data Sets of Jöri and Jungfrauoch

Model No.	Jöri ^a			Jungfrauoch ^b		
	MBE	RMSE	r^2	MBE	RMSE	r^2
1	5.8	14.1	0.88	3.4	16.1	0.80
2	10.4	16.6	0.80	4.1	18.1	0.74
3	6.6	20.1	0.46	6.7	27.3	-0.25
4	-11.7	20.5	0.77	-24.2	23.0	0.68

^aJöri Lakes data set (2520 m a.s.l.).

^bJungfrauoch data set (3580 m a.s.l.).

ASRB project by the PMOD/WRC at Jungfrauoch (3580 m a.s.l.). It contained 360 data points from 1997 for model verification.

The results obtained with the Jöri—and the Jungfrauoch—data are similar to the ones from the PMOD/WRC data set (Table 5). Model 1 clearly gives the most accurate description of the independent data sets as seen in the lowest RMSE, the highest r^2 , and an MBE that is closest to 0 Wm^{-2} . The order of performance of the models is the same as for the PMOD/WRC data set, with model 2 yielding better results than models 3 and 4. The low and even negative r^2 for model 3 (Table 6) indicate that it is not usable for these high-mountain sites. The weak performance of model 4 can largely be attributed to an inadequate cloud cover parameterization. If the variable a of Equation (7) would be set to 0.49 for the Jungfrauoch data set as proposed above, model 4 would improve enormously ($r^2 = 0.89$, $\text{MBE} = 0.2 \text{ Wm}^{-2}$, $\text{RMSE} = 17.1 \text{ Wm}^{-2}$). It is not yet clear how the variable a can be defined correctly for each site without appropriate calibration.

Seasonal Performance of the Models

The MBE and the RMSE for the Jöri data set were also calculated independently for each season (Table 7). All models except number 2 express distinct seasonal variations of MBE. Models 3 and 4 exhibit an MBE far from 0 Wm^{-2} , especially during the winter, when MBE was calculated to be close to 0 Wm^{-2} for model 1. This pattern reverses in summer, with model 1 producing MBEs far from 0 Wm^{-2} . Models 3 and 4 are not able to correctly parameterize incoming longwave radiation under cold and dry atmospheric conditions. Thorough analysis of the seasonal variation of MBE for model 1 showed that it underestimates incoming longwave radiation mainly for partly cloudy days in late summer when the snow cover around the Jöri station had disappeared. Because of multiple reflections between the sky and the snow cover, the calculated clearness index K_0 is usually higher for cloudy conditions in winter than for the snow-free summer. Other models calculating incoming longwave radiation as a function of global radiation (Aubinet, 1994; Ineichen et

Table 6. Correlation between Measured and Calculated Incoming Longwave Radiation of the Four Tested Models and Verification Data Sets

Model Nr.	r^2 Jöri ^a	r^2 JFJ ^b
1	0.88	0.80
2	0.80	0.74
3	0.46	-0.25
4	0.77	0.68

^aJöri Lakes data set (2520 m a.s.l.).^bJungfrauoch data set (3580 m a.s.l.).

al., 1984) are based on lowland data and are expected to yield less precise results for sites where snow cover is an important determinant. For all tested models, RMSE varies only slightly with season and not as distinctly as MBE does. RMSE are therefore less suited to explain seasonal differences.

Applicability and Limitations of the New Model

In general, the new model describes incoming longwave radiation in high-mountain environments well. It also performed reasonably well at one lowland station. However, the new model is expected to yield larger errors at sites where high water vapor pressure is common, such as in the tropics. In its present formulation, the new model can only calculate daily means of incoming longwave radiation. The new model yields slightly smaller RMSE in the summer months because of longer sunshine duration and therefore better indication of cloud cover. Cloud cover during the night cannot be represented. Consequently, long nights limit the performance of the model. Nevertheless, the model yielded good results for the Jöri site, where around the winter solstice only 2 hours of direct sunlight was recorded on cloudless days. For sites at high latitudes or with complete terrain shading in winter, the new model is not applicable because the cloud cover information extracted from the global radiation measurements is not available without direct sunlight. For the new model, it is also important that global radiation measurements are reasonably accurate. Erroneous global radiation measurements—e.g., when sensors are snow covered—will affect the calculation of the clearness index and cause large errors in incoming longwave radiation calculation.

CONCLUSIONS

A new model is presented for the calculation of daily average incoming longwave radiation in high-mountain as well as lowland sites. It is a function of air temperature, relative humidity, and global radiation. The model was calibrated using a highly accurate data set measured by the PMOD/WRC. The data set included daily mean values from two high-mountain stations and one lowland site. The new

Table 7. Comparative Statistics of the Jöri Data for Different Seasons

Model	MBE				RMSE			
	Winter ^a	Spring ^b	Summer ^c	Fall ^d	Winter ^a	Spring ^b	Summer ^c	Fall ^d
1	2.6	0.0	11.1	6.1	12.3	13.5	11.8	15.4
2	10.4	11.7	12.0	7.1	13.1	18.0	14.9	18.7
3	15.0	8.1	0.9	4.1	19.9	20.6	16.0	21.1
4	-19.7	-16.5	-0.6	-14.9	14.6	22.0	17.4	20.9

^aMonths December to February.

^bMonths March to May.

^cMonths June to August.

^dMonths September to November.

model was verified with data from the Jöri lakes, a high-mountain lake research site and with data from Jungfraujoch, an ASRB site. The longwave parameterization models by Konzelmann et al. (1994), Idso and Jackson (1969), and Brutsaert (1975) were also tested with the same data sets and compared to the new model.

The new model, applied to high altitude sites, is superior to the existing ones for daily mean values. It is also applicable to winter situations when only a few hours of global radiation measurements are available for the whole day. In order for a model to be suitable for a certain site or application, the RMSE has to be as small as possible and the MBE should be close to 0 Wm⁻². The new model, when applied to independent high-mountain data sets, yielded the smallest RMSE and a MBE closest to 0 Wm⁻². From the already existing models, the one by Konzelmann et al. (1994) generally yielded the best results. It is difficult, however, to draw general conclusions about the suitability of the tested models, because they were developed for different sites, cloud conditions, and seasons. The new model yielded the most consistent results, and the performance was reasonable for all cloud conditions, sites, and seasons. Model 2 did not perform well under cloudless conditions, whereas models 3 and 4 were not suitable for high-mountain conditions. The latter two models also perform less well under overcast conditions, an effect that can be attributed to an inadequate cloud cover parameterization.

The model presented in this study is a viable substitute for the previous models requiring cloud cover information as input data, which cannot be observed in automatically. The use of global radiation in place of cloud cover has the advantage that it is one of the most widely measured parameters at automated (unmanned) weather stations. Therefore, the new model is suitable for remote sites such as high-mountain environments, which are normally far from weather observation posts.

Acknowledgments: This research was supported by the EU Environment and Climate Program (project MOLAR NO. ENV4-CT95-0007), financed by the Ministry of Education and Science of Switzerland (contract No. BBW 95.0518-2) and by the Swiss National Science Foundation Grant (CLEAR No. 5001-44614/1). Data were provided by the PMOD/WRC, where recorded within the ASRB project. The ASRB-project was financed by the Swiss National Science Foundation Grant (No. 4031-033356) and by

ETH Grant (No. 41-2711.5). The assistance of Hanspeter Schmidhauser and Alfons Birchmeier in the maintenance of the Jöri research station is gratefully acknowledged. We thank Donat Högl for the data acquisition at Jöri and Armand Vernez for the meteorological sensors. All cloud cover data were provided by the Swiss Meteorological Institute.

BIBLIOGRAPHY

- Aubinet, M. (1994) Longwave sky radiation parameterizations. *Solar Energy*, Vol. 53, 147–154.
- Barry, R. G. (1992) *Mountain Weather and Climate*. New York, NY: Routledge.
- Berdahl, P. and Martin, M. (1984) Emissivity of clear skies. *Solar Energy*, Vol. 32, 663–664.
- Bolz, H. M. (1949) Die Abhängigkeit der infraroten Gegenstrahlung von der Bewölkung (The dependence of infrared counter-radiation on cloud cover). *Zeitschrift für Meteorologie*, Vol. 3, 201–203.
- Brutsaert, W., (1975) On a derivable formula for longwave radiation from clear skies. *Water Resources Research*, Vol. 11, 742–744.
- Brutsaert, W., (1982) *Evaporation into the Atmosphere*. Dordrecht, The Netherlands: Reidel Publishing Company.
- Gabathuler, M. (1999) Physical Ecosystem Determinants in High Mountain Lakes. The Jöri Lakes, Switzerland. Unpublished Ph.D. thesis, ETH Zürich, Switzerland.
- Greuell, W., Knap, W. H., and Smeets, P.C. (1997) Elevational changes in meteorological variables along a midlatitude glacier during summer. *Journal of Geophysical Research*, Vol. 102, 25,941–25,954.
- Idso, S. B. and Jackson, R. D. (1969) Thermal radiation from the atmosphere. *Journal of Geophysical Research*, Vol. 74, 5397–5403.
- Ineichen, P., Gremaud, M., Guisan, O. and Mermoud, A. (1984). Infrared sky radiation in Geneva. *Solar Energy*, Vol. 32, 537–545.
- Kondratyev, K. Y. (1973) *Radiation Characteristics of the Atmosphere and the Earth's Surface*. New Delhi, India: Amerind Publishing Co.
- Konzelmann, T., Vandewal, R. S. W., Greuell, W., Bintanja, R., Henneken, E. A. C., and Abeouchi, A. (1994) Parameterization of global and longwave incoming radiation for the Greenland ice-sheet. *Global and Planetary Change*, Vol. 9, 143–164.
- Liston, G. E. and Hall, D. K. (1995) An energy balance model of lake ice evolution. *Journal of Glaciology*, 41, 373–382.
- Livingstone, D. M. and Imboden, D. M. (1989) Annual balance and equilibrium temperature of Lake Aegeri, Switzerland. *Aquatic Sciences*, Vol. 51, 351–369.
- Marti, D. E. and Imboden, D. M. (1986) Thermische Energieflüsse an der Wasseroberfläche: Beispiel Sempachersee (Thermal energy flows at the water surface: Lake Sempach as an example). *Aquatic Sciences*, Vol. 48, 196–229.
- Marty, C. A. (2000) Surface Radiation, Cloud Forcing and Greenhouse Effect in the Swiss Alps. Unpublished Ph.D. thesis, ETH Zürich, Switzerland.
- Oke, T. R. (1987) *Boundary Layer Climates*. New York, NY: Methuen.
- Olyphant, A. (1986) Longwave radiation in mountainous areas and its influence on the energy balance of alpine snowfields. *Water Resources Research*, Vol. 22, 62–66.

- Philipona, R., Marty, C., and Fröhlich, C. (1996) Measurements of the longwave radiation budget in the Alps, IRS96. In W. L. Smith and K. Stamnes, eds., *Current Problems in Atmospheric Radiation*. Hampton Roads, VA: Deepak Publishing, 786–789.
- Saunders, I. R. and Bailey, W. G. (1997) Longwave radiation modeling in mountainous environments. *Physical Geography*, Vol. 18, 37–52.
- Swinbank, W. C. (1963) Longwave radiation from clear skies. *Quarterly Journal of the Royal Meteorological Society*, Vol. 89, 339–348.